MICROSCOPIC DRYING BEHAVIOUR OF A PAPER SHEET IN A MULTI-CYLINDER DRYER

W.Jan Coumans and Bram J. Ramakers

Eindhoven University of Technology, Laboratory of Separation Technology and Transport Phenomena, P.O. Box 513, 5600 MB Eindhoven, The Netherlands,
E-mail: w.j.coumans@tue.nl

Keywords: paper, multi-cylinder dryer, diffusion, modelling, porous, conductive/convective drying

ABSTRACT

Transport phenomena inside a paper sheet undergoing alternating boundary conditions in a multi-cylinder paper dryer are studied. The physical-mathematical modelling is based on a description of the microscopic transport mechanisms in a porous material, e.g. Darcy flow for liquid flow due to capillary forces, vapour diffusion due to a vapour pressure gradient, heat flow as a result of the mass flow and a temperature gradient and solids flow due to a decrease of the moisture content (volume shrinkage). Also the development of internal gas pressure gradients are taken into account.

The partial differential equations are solved by using the NAG®-Fortran library called by a user-friendly interface program created with Borland Delphi® IV programming language. Simulations yield moisture profiles, temperature profiles and gaseous pressure profiles in the thickness direction of a sheet of paper or cardboard during its course through a multi-cylinder dryer.

So far two interesting phenomena could be observed: at high temperature gradients and/or pressure gradients moisture may be accumulating in the centre part of the sheet leading to moisture contents *higher* than the initial value. Under certain drying conditions a small underpressure of the gaseous phase in the sheet may be developed. These observations and the results of some simulations will be discussed.

INTRODUCTION

The modelling of a multi-cylinder dryer is not an easy task. Depending on the aims one can deal with this problem at several levels of scale and physical refinement. Some interesting approaches are given in literature by Asensio & Seyed-Yagoobi (1992, 1993), Harrmann & Schulz (1990) and most recently by Ramaswamy & Holm (1999) and Reardon et.al. (1999).

The focus in this study is mainly directed towards the transport phenomena *inside* a porous layer during a drying process with alternating boundary conditions. These types of studies are quite hard if not impossible to be carried out experimentally under practical industrial drying conditions. So, one has to resort to modelling and simulation followed by validation via small scale and dedicated laboratory experiments with well-known boundary conditions for the drying sheet.

In a real dryer it may be expected that the external conditions depend on the position in the dryer, especially the length direction. However, for the time being it is assumed that the drying air in the hood has a constant temperature and humidity, and that the steam temperature is the same for all cylinders in the dryer. The paper sheet is considered as a porous material, in which several mechanisms for mass and heat transfer in the porous microstructure play a role. Shrinkage of the paper thickness is taken into account. In a former study the set of ruling equations has been developed and the properties of cardboard have been measured extensively (Kruf, 1992; Coumans and Kruf, 1995). In the current research (Ramakers, 1999) the model has been refined and extended and a more user-friendly computer program is developed. For a given set of data for paper sheet properties, process conditions and dryer configuration the program delivers the profiles of moisture content, temperature and gaseous pressure at any moment during the drying process.

INTERNAL TRANSPORT PHENOMENA

A saturated paper sheet consists of a porous web of fibres forming a solid matrix (s), whereby the voids between the fibres are fully filled up with liquid water (ℓ). In case of undersaturation the voids are partially filled up with liquid water and partially with a gaseous phase (g), consisting of water vapour (v) and air (a). Though moisture and temperature gradients will build up in the length direction of the sheet, all transport phenomena can be considered as taking place in the thickness direction only. Also shrinkage of the sheet will take place dominantly in this direction. Shrinkage is characterised by the empirical relation between the dry solids concentration (ρ_s) and the moisture content (u). The mass balances for solid, water and air and the heat balance form the basis of a microscopic model. The solids mass balance is accounted for by introducing the so-called solids space co-ordinate (z) by $dz = \rho_s \cdot dr$. Note that z is expressed in kg solid/m^2, a unit being quite familiar in paper technology. The water and air mass balances can be written as (Coumans et.al., 1994):

$$\left(\frac{\partial u}{\partial t}\right)_z = -\left(\frac{\partial j_w^s}{\partial z}\right)_t \qquad \text{and} \qquad \left(\frac{\partial a}{\partial t}\right)_z = -\left(\frac{\partial j_a^s}{\partial z}\right)_t \tag{1}$$

and the enthalpy balance by:

$$\left(\frac{\partial H}{\partial t}\right)_z = -\left(\frac{\partial q^s}{\partial z}\right)_t \tag{2}$$

All fluxes in the above equations are defined with respect to the solids velocity (hence superscript s). It is assumed here that water present inside the fibres does not contribute substantially to the total moisture flux, and thus:

$$j_w^s \approx j_\ell^s + j_v^s \tag{3}$$

The liquid water flux is given by Darcy's law:

$$j_\ell^s = -d_\ell \frac{K_\ell}{\eta_\ell}\frac{\partial P_\ell}{\partial r} \qquad \text{with} \quad P_\ell = P - P_c \tag{4}$$

As the internal gaseous phase is a binary mixture of water vapour and air the following equation applies to the vapour flux:

$$j_v^s = \left(j_v^s + j_a^s\right)\omega_v - D\rho'\frac{\partial \omega_v}{\partial r} \tag{5}$$

The total gas flux ($j_v^s + j_a^s$) can be described by Darcy's law:

$$j_v^s + j_a^s = -\rho'\frac{K_g}{\eta_g}\frac{\partial P}{\partial r} \tag{6}$$

Analogue equations hold for the air flux j_a^s. The enthalpy flux q^s depends on the mass fluxes and the Fourier heat conduction flux:

$$q^s \approx j_\ell^s h_\ell + j_v^s h_v - \lambda_{eff}\frac{\partial T}{\partial r} \tag{7}$$

where the enthalpy flux associated with the air flux is neglected.

After transforming all these flux expressions in terms of the solids space co-ordinate (z), the solids based moisture content (u) and by evaluating all driving forces in terms of ($\partial u/\partial z$), ($\partial T/\partial z$) and ($\partial P/\partial z$) the following set of 4 flux equations is obtained:

$$j_l^s = -L_u \cdot \frac{\partial u}{\partial z} - L_T \cdot \frac{\partial T}{\partial z} - L_P \cdot \frac{\partial P}{\partial z} \tag{8}$$

$$j_v^s = -V_u \cdot \frac{\partial u}{\partial z} - V_T \cdot \frac{\partial T}{\partial z} - V_P \cdot \frac{\partial P}{\partial z} \tag{9}$$

$$j_a^s = -A_u \cdot \frac{\partial u}{\partial z} - A_T \cdot \frac{\partial T}{\partial z} - A_P \cdot \frac{\partial P}{\partial z} \tag{10}$$

$$q^s \approx j_\ell^s \cdot h_\ell + j_v^s \cdot h_v - \lambda_{eff} \cdot \rho_s \cdot \frac{\partial T}{\partial z} \tag{11}$$

where the 9 lump coefficients are given by:

$$L_u = -\rho_s \cdot d_\ell \cdot \frac{K_\ell}{\eta_\ell} \cdot \frac{\partial P_c}{\partial u} \tag{12}$$

$$L_T = -\rho_s \cdot d_\ell \cdot \frac{K_\ell}{\eta_\ell} \cdot \frac{\partial P_c}{\partial T} \tag{13}$$

$$L_P = \rho_s \cdot d_\ell \cdot \frac{K_\ell}{\eta_\ell} \tag{14}$$

$$V_u = \rho_s \cdot D_{eff} \cdot \frac{M_a}{\widetilde{M}} \cdot \frac{P_v M_w}{RT} \cdot \frac{\partial \ln(a_w)}{\partial u} \tag{15}$$

$$V_T = \rho_s \cdot D_{eff} \cdot \frac{M_a}{\widetilde{M}} \cdot \frac{P_v M_w}{RT} \cdot \left[\frac{\partial \ln(a_w)}{\partial T} + \frac{\partial \ln\left(P_v^o\right)}{\partial T}\right] \tag{16}$$

$$V_P = \rho_s \cdot \frac{P_v M_w}{RT} \cdot \left[\frac{K_g}{\eta_g} - D_{eff} \cdot \frac{M_a}{\tilde{M}} \cdot \frac{1}{P} \right] \quad (17)$$

$$A_u = -\rho_s \cdot D_{eff} \cdot \frac{M_a}{\tilde{M}} \cdot \frac{P_v M_w}{RT} \cdot \frac{\partial \ln(a_w)}{\partial u} \quad (18)$$

$$A_T = -\rho_s \cdot D_{eff} \cdot \frac{M_a}{\tilde{M}} \cdot \frac{P_v M_w}{RT} \cdot \left[\frac{\partial \ln(a_w)}{\partial T} + \frac{\partial \ln\left(P_v^o\right)}{\partial T} \right] \quad (19)$$

$$A_P = -\rho_s \cdot \left[D_{eff} \cdot \frac{M_a}{\tilde{M}} \cdot \frac{P_v M_w}{RT} \cdot \frac{1}{P} - \frac{(P - P_v) M_a}{RT} \cdot \frac{K_g}{\eta_g} \right] \quad (20)$$

All these lump coefficients are functions of P, T and u, which follow eventually from physical properties of the paper sheet, such as sorption isotherm, permeability for gas and liquid, porosity, shrinkage, etc. To obtain all these properties dedicated and laborious experiments are needed. It goes beyond the scope of this paper to explain all the details.

INITIAL AND BOUNDARY CONDITIONS

During drying of paper or board in a multi-cylinder dryer the sheet is rolling on and off the cylinders, causing cyclic and alternating boundary conditions. A dryer felt (or dryer fabric) assures an intimate contact between the sheet and the cylinder wall. According to Nissan et.al. (1955) four drying stages can be distinguished at each cylinder (Figure 1). During phases I and III one side of the sheet is in contact with the cylinder wall while the other side is in free contact with the surrounding air. In phase II there is no free contact with the air, because now there is an extra resistance to mass and heat transport from the dryer felt. In phase IV, where the sheet traverses to the next cylinder both sides are in free contact with the air (free draw). For all drying stages the boundary moisture flux can be described by:

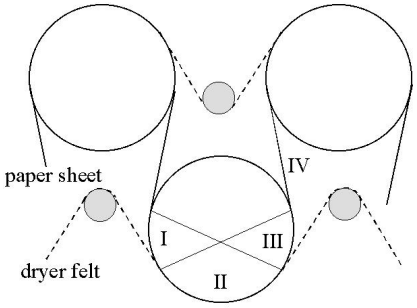

Figure 1: Basic principle of a multi-cylinder dryer.

$$j^s_{w,i} = j^s_{v,i} + j^s_{\ell,i} = k \cdot \frac{M_w P_t}{RT_f} \cdot \ln\left(\frac{P_t - P_{v,\infty}}{P_t - P_{v,i}} \right) \quad (21)$$

the boundary enthalpy flux by:

$$q^s = \alpha \cdot (T_i - T_\infty) + j^s_{w,i} \cdot h_v \quad (22)$$

and for the boundary pressure holds:

$$P_i = P_t \quad (23)$$

For each drying stage the boundary condition is defined by values for k, α, $P_{v\infty}$ and T_∞.

In case the paper boundary is in contact with the cylinder wall the boundary moisture flux is assumed to be zero, which can be expressed by putting k=0 and $P_{v,\infty}$=0. With respect to the enthalpy flux T_∞=T_{steam} is taken and the heat transfer coefficient α is the overall result of steam condensation inside the cylinder, heat conduction through the cylinder wall and the contact layer respectively.

In case the paper boundary is in free contact with the drying air k and α follow from Sherwood/Nusselt correlations. If the dryer felt is covering the paper sheet, these values are corrected for this extra resistance by a simple series/parallel model. Now $P_{v,\infty}$ and T_∞ refer to the conditions of the drying air.

As the initial conditions uniform profiles for u, T and P are chosen, thus $u=u_0$, $T=T_0$ and $P=P_t$ for all values of the space co-ordinate z.

NUMERICAL MODEL

The above set of 3 non-linear parabolic partial differential equations (1-2), including the 4 flux equations (8-11) and 9 lump coefficients (12-20), can be solved numerically for the given boundary conditions (21-23) and initial conditions by using routine D03PCF from the NAG®-Fortran-library (1998). The NAG® routine is attached to a Borland Delphi® IV program as an external 'dll-file'. Delphi® IV uses object oriented Pascal, which enables a user-friendly environment for the input and output of the simulations. Any satisfying space grid can be defined; if desired, a denser grid at the boundaries is obtained by specifying a mesh-factor. Time steps are automatically chosen by the routine itself depending on the desired accuracy. The numerical solution provides profiles of moisture (u), temperature (T) and pressure (P) in the thickness direction of the paper sheet (z) at any moment (t).

PROPERTIES AND CONDITIONS

Below an overview is given of the data needed for the computer program. Between brackets typical values for the simulation runs are given. Because of limited space not all details can be presented here (Ramakers, 1999). The material studied here was cardboard from Beukema & Co.

Properties of paper/board sheet:

- sorption isotherm: $a_w=a_w(u,T)$
- capillary pressure: $P_c=P_c(u,T)$
- permeability for liquid and gas: $K_\ell=K_\ell(u,T)$ and $K_g=K_g(u,T)$
- vapour diffusion coefficient: $D_{eff}=D_{eff}(u,T,P)$
- shrinkage curve: $\rho_s=\rho_s(u)$
- fibre saturation point (0.44 kg w/kg ds)
- true solids density (1430 kg/m^3)
- dry paper density (735 kg/m^3)
- heat capacity of solid (1340 J/kg °C)
- basis weight (800 g/m^2 or 80 g/m^2)
- initial conditions:
  u_0=0.5 or 1 kg w/kg ds, T_0=35 °C, P_0=1 bar

Thermal-physical properties of:

- air
- water (liquid, vapour)

Machine parameters:

- number of cylinders (1 and 65)
- diameter of cylinder (1.50 m)
- fraction of cylinder surface covered by paper sheet (0.75)
- fraction of cylinder surface covered by paper sheet + dryer felt (0.68)
- length of free draw between cylinders (2.80 m)
- dimensions of dryer felt

Process conditions:

- temperature drying air (73 °C)
- dew point drying air (25 °C)
- temperature of steam (120 °C or 140 °C)
- ambient pressure (1 atm)
- velocity of paper sheet through dryer (0.58 m/s)
- conductive heat transport coefficients:
  α_{steam}=5000, α_{cyl}=2000, $\alpha_{contact}$=150 W/m^2 °C

SIMULATIONS

The computer program enables the study of a multi-cylinder drying process by simulations at different machine configurations, process conditions and properties of the paper/board. Parameters to control the numerical calculation are number of grid points, mesh factor, relative error in time and time interval for output. Here 3 examples of simulations are given.

Table 1: Overview of simulations (parameters being varied in simulations are coloured blue).

Simulation No.→	1	2	3
Basis weight (kg/m^2)	0.8	0.8	0.8
Thickness of dry sheet (mm)	1.5	1.5	1.5
Number of cylinders	1	65	1
Diameter of cylinder (m)	1.5	1.5	1.5
Speed of paper/board sheet (m/s)	0.58	0.58	0.58
Steam temperature (°C)	120	120	140
Initial moisture content (kg w/kg ds)	0.5	0.5	1
Air temperature (°C)	73	73	73
Dew point air (°C)	25	25	25
Initial temperature paper (°C)	35	35	50
α_{steam} (W/m^2 °C)	5000	5000	5000
α_{wall} (W/m^2 °C)	2000	2000	2000
$\alpha_{contact}$ (W/m^2 °C)	150	150	1000
Number of grid points	51	171	51
CPU time (min:sec)[1]	00:10	11:23	00:16
Error in time (%)	1e-4	1e-5	1e-4

[1]The CPU time is obtained with a Pentium® III processor, 500 MHz and 128 Mb RAM.

Simulation 1

In this simulation the drying behaviour only on the first cylinder is studied (see Figures 2a-d). Under the given conditions of sheet speed and cylinder diameter etc. it simply follows that the contact time of the sheet with the cylinder wall is 6.1 seconds (drying stages I, II and III), all 4 drying stages take in total 10.9 seconds. As can be seen in Figure 2c the temperature of the sheet boundary in contact with the hot cylinder wall rises within the 6 seconds from 35 to about 80 °C. During the free draw (stage IV) this

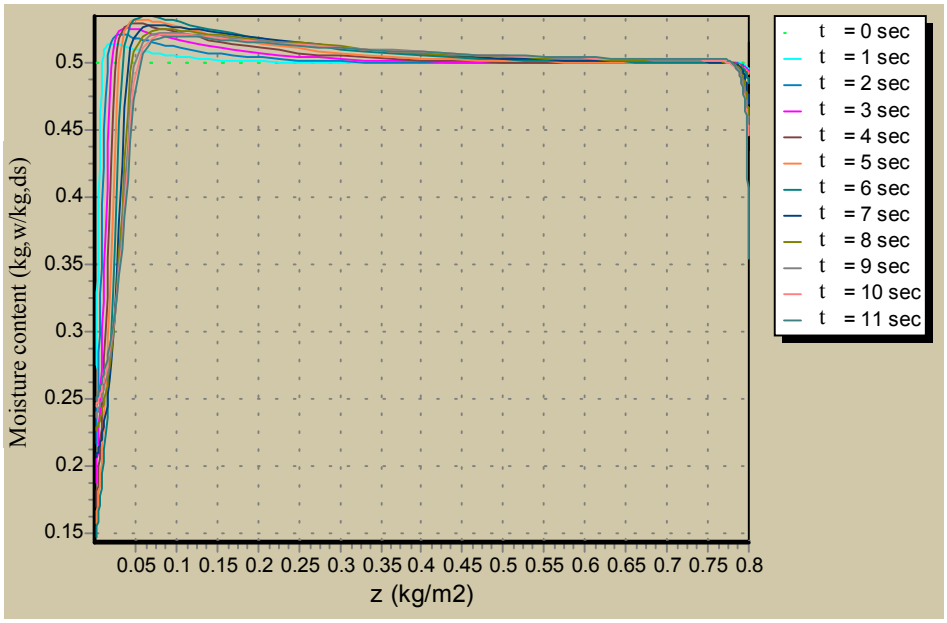

Figure 2a: Moisture profiles from simulation 1.

temperature decreases. The profile at 11 seconds shows that the other side of the sheet has briefly contacted the hot surface of the 2nd cylinder. Moisture profiles (Figure 2a) show that the moisture at the wall side is pushed towards the centre of the sheet, where the moisture content rises above its initial

value. Because boiling is not possible at these temperature levels, this effect must be due to the strong temperature gradients. A small but clear drying effect takes place on the right side of the sheet (Figure 2a); the drying effect appears to take place mainly during drying stage IV (Figure 2b). Figure 2d shows that during the first 6 seconds the pressure inside the sheet at the wall side increases slightly up to 1100 Pa. In drying stage IV the pressure drops suddenly and both sheet boundaries have ambient pressure. In the left part of the sheet the pressure drops quickly, because the gaseous phase can escape easily and because the temperature decreases; this may lead in a certain region of the sheet to a temporary slight underpressure. The simulation shows that the error in the mass balance is 0.15% and in the enthalpy balance 0.72%.

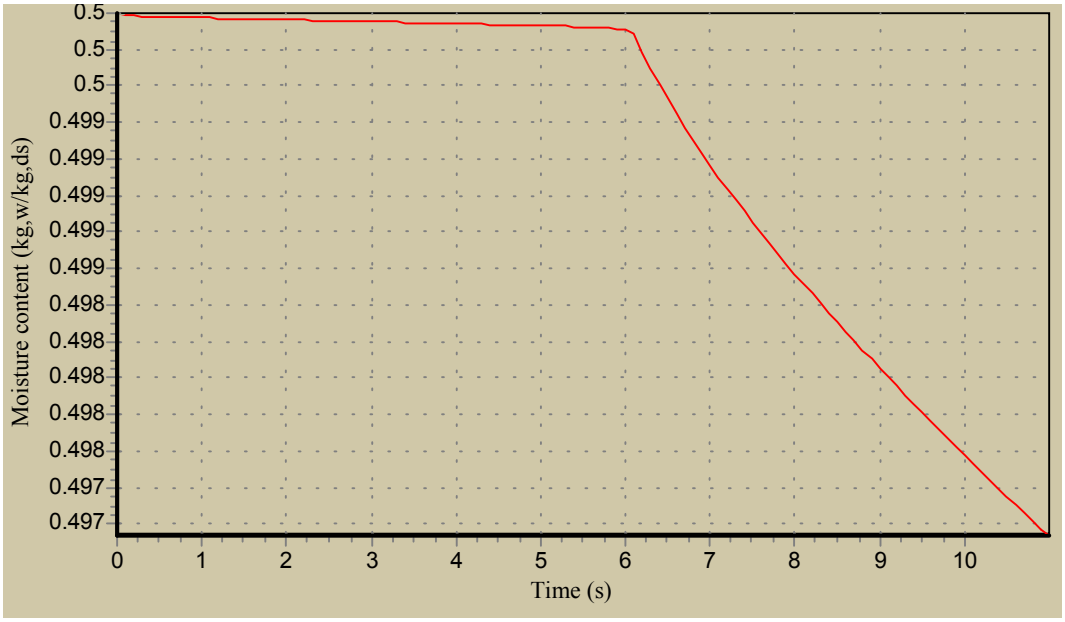

Figure 2b: Averaged moisture content versus time from simulation 1.

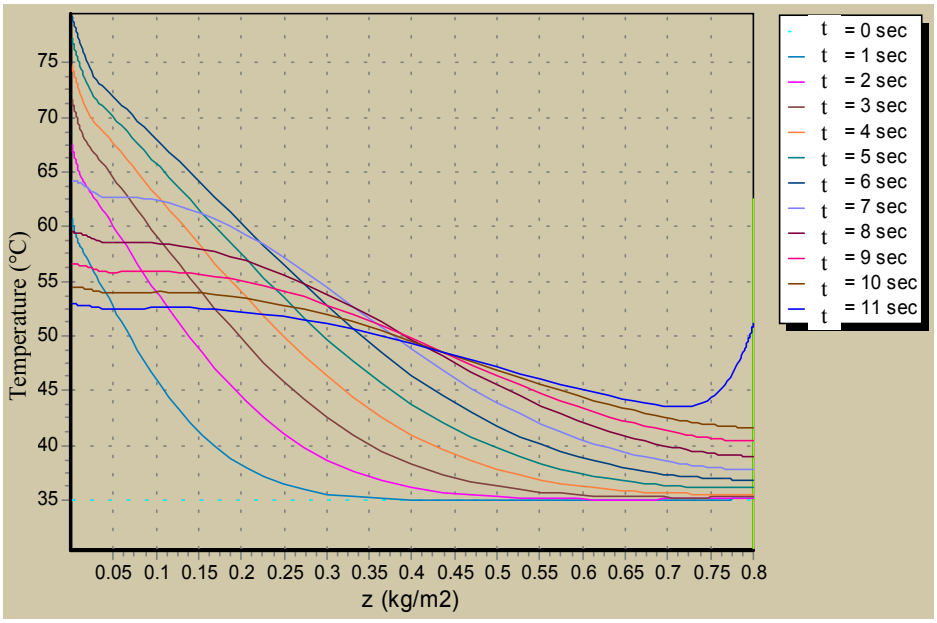

Figure 2c: Temperature profiles from simulation 1.

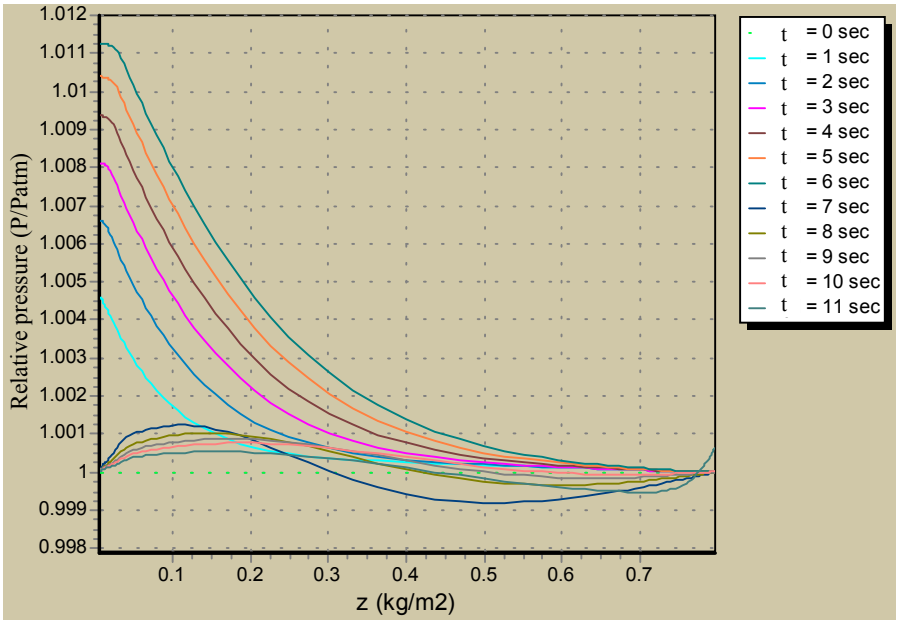

Figure 2d: Pressure profiles from simulation 1.

Simulation 2

In this simulation the drying behaviour of the sheet is followed during its course through a dryer consisting of 65 cylinders. In Figure 3a the evolution of moisture profiles is shown with intervals of 44

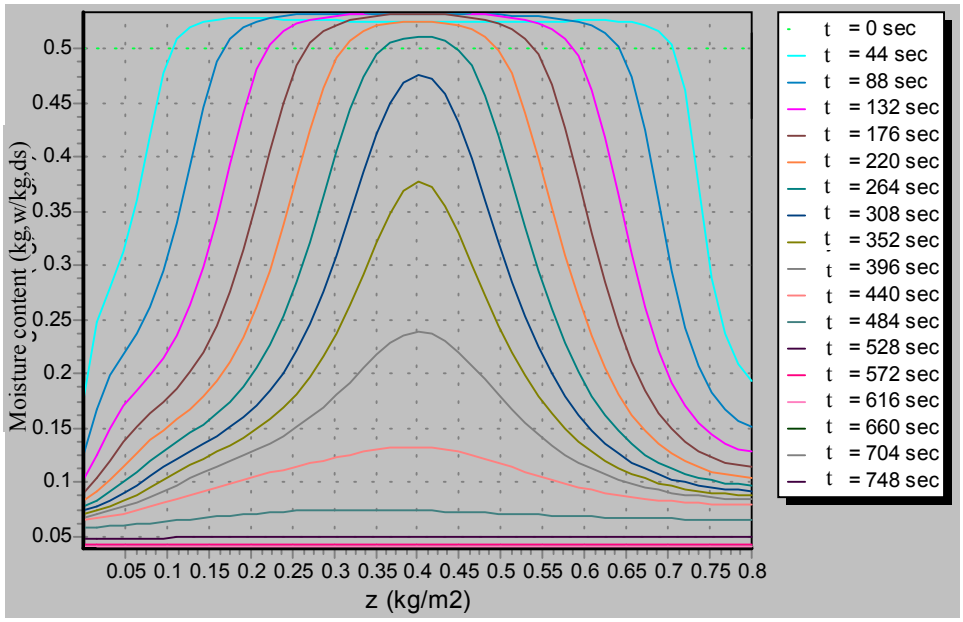

Figure 3a: Moisture profiles taken at intervals of 44 seconds from simulation 2.

seconds (≅4 cylinders). Clearly can be seen how in the beginning the water is pushed to the centre of the sheet, thereby causing a moisture-content in the centre being higher than the initial value. Both sides of the sheet experience the same alternating boundary conditions and averaged in time the drying behaviour is symmetric. However, this symmetry in moisture profile will not necessarily be found at any arbitrarily moment. Bell-shaped moisture profiles are found, which is to be expected for porous material where moisture transport takes place by liquid flow and vapour diffusion. During the first 3-4 cylinders the

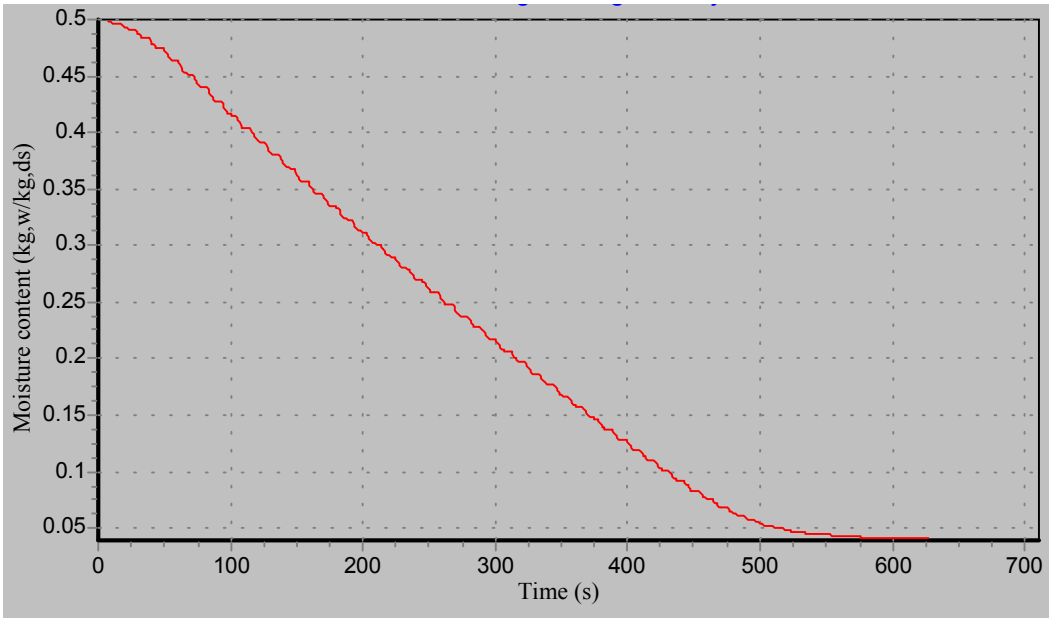

Figure 3b: The averaged moisture content versus time in a 65-cylinder dryer from simulation 2.

drying effect is rather low (Figure 3b). After this period there is a nearly linear decrease of the averaged moisture content versus time. Finally, the moisture content tends to the equilibrium value of 0.0396 kg w/kg ds. In case a final moisture-content of 0.06 kg w/kg ds is desired one observes, that this value is reached after 480 seconds, which corresponds with 44 cylinders.

The averaged temperature of the sheet is also oscillating because of the alternating boundary conditions. After 4-5 cylinders this oscillation stabilises at a temperature level of about 75 °C. It seems as if a sort of steady-state is obtained, where the heat delivered to the sheet is completely used for evaporation of water; drying rate and heat flow rate keep nearly constant in this period. Once the equilibrium moisture content is reached the temperature increases again and tends to 115 °C (concluded form another simulation), a value somewhere in between the temperatures of the steam (120 °C) and drying air (73 °C).

Similarly, the averaged pressure in the sheet also oscillates (Figure 3d). The simulation shows that the error in the mass balance is 0.10% and in the enthalpy balance 0.60%.

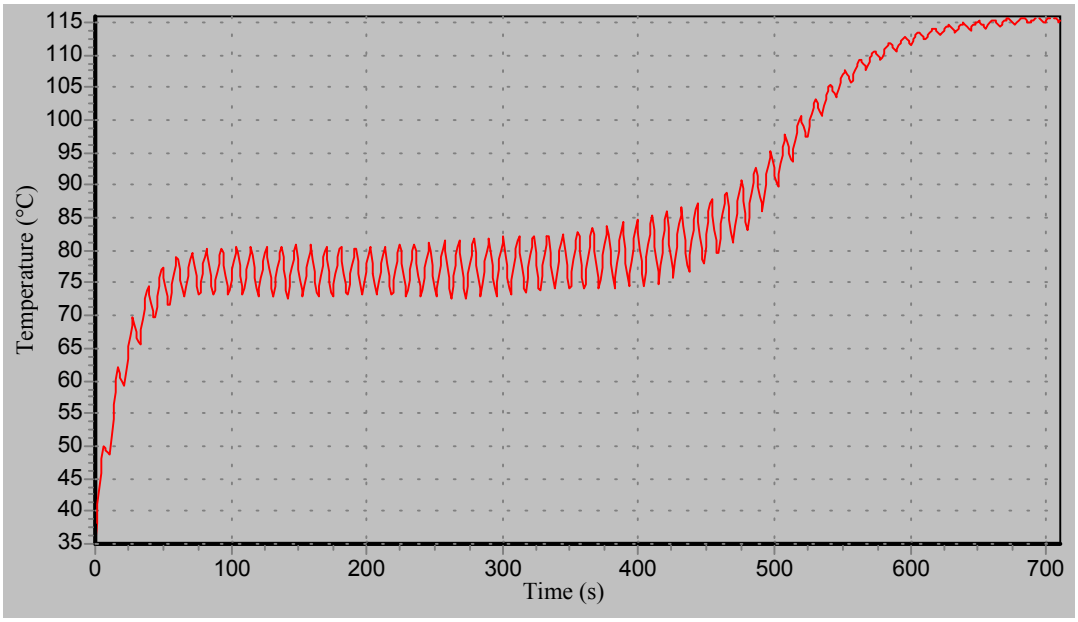

Figure 3c: Averaged temperature from simulation 2 versus time.

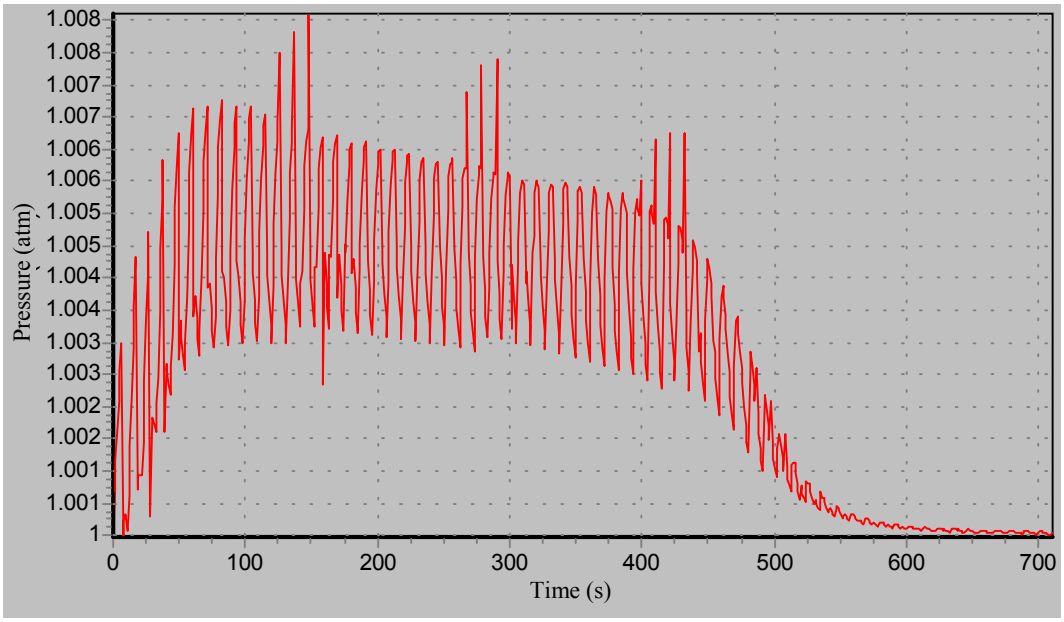

Figure 3d: Averaged gaseous pressure from simulation 2 versus time.

Simulation 3

At high steam temperatures boiling phenomena may be expected inside the sheet. In this simulation boiling is provoked by choosing a high steam temperature (140 °C), a high initial moisture content (1.0 kg w/kg ds), a high initial sheet temperature (50 °C) and a better contact between sheet and cylinder wall ($\alpha_{contact}$=1000 W/m^2 °C).

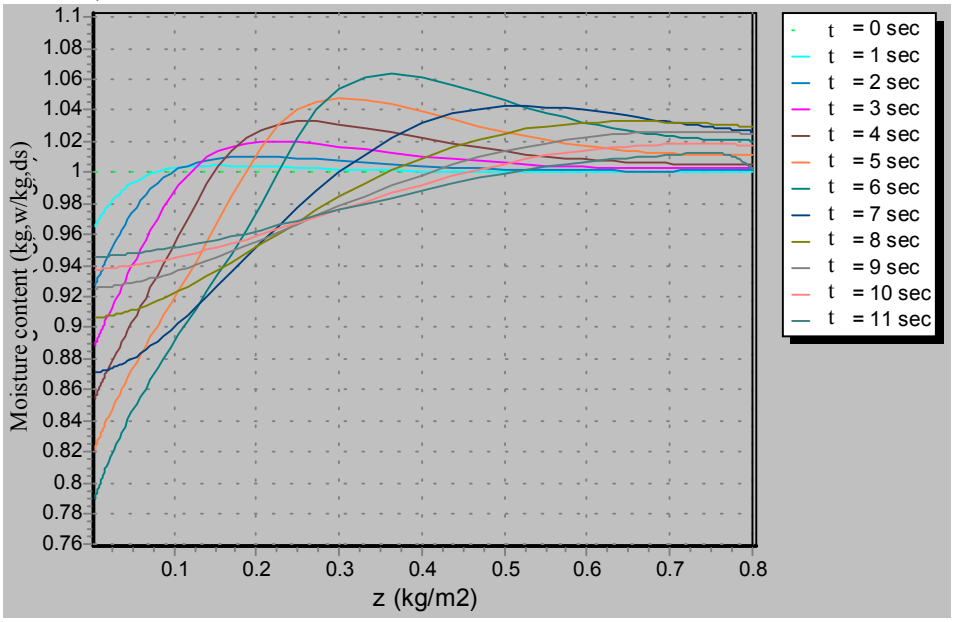

Figure 4a: Moisture profiles (zoomed in) from simulation 3.
Moisture is clearly driven to the centre of the material.

Figure 4a shows the moisture profiles, now strongly pushed inwards during the first 6 seconds. Indeed, under these conditions the temperature of the sheet at the interface rises up to 106 °C and thus exceeds clearly the atmospheric boiling temperature (Figure 4b). Because the vapour can not escape directly via the nearby surface, the pressure builds up to 1.26 atm (Figure 4c), which is in agreement with a boiling

temperature of 106 °C. This pressure is the major driving force in pushing the water to the centre of the sheet.

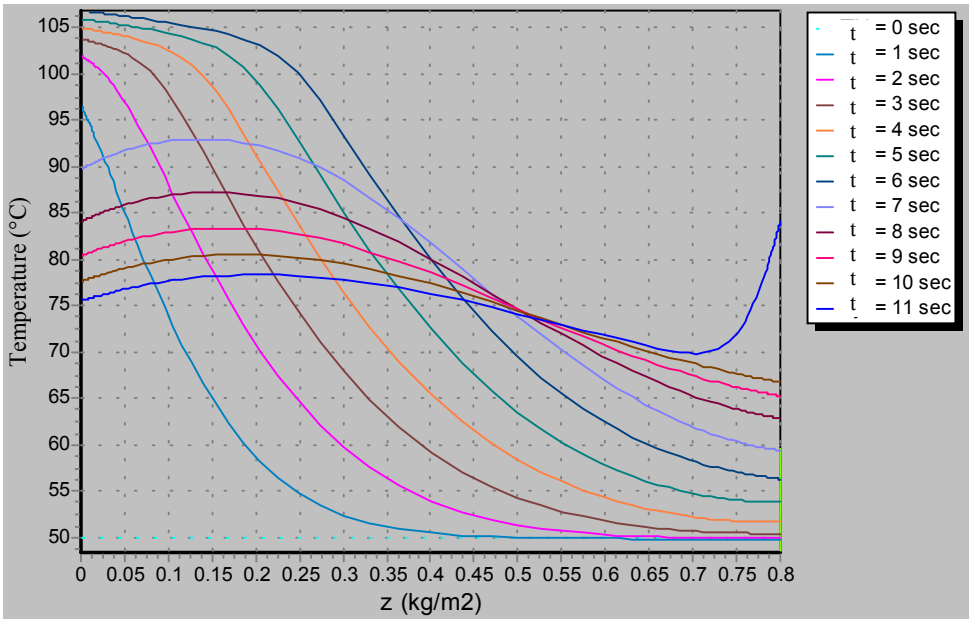

Figure 4b: Temperature profiles from simulation 3. Note that near the interface temperature exceeds the boiling point of water.

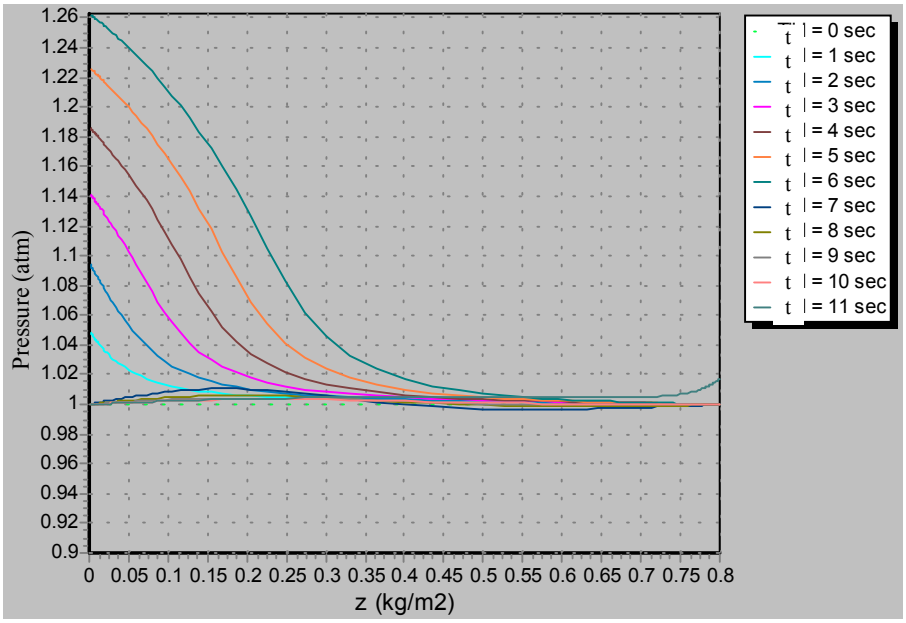

Figure 4c: Pressure profiles from simulation 3. Note that now the gas pressure clearly exceeds atmospheric pressure.

CONCLUSIONS

A generalised model for the microscopic drying behaviour of a porous layer subjected to alternating boundary conditions is briefly presented. This model forms the core of a computer model enabling the simulation of the drying of paper and cardboard in a (standard) multi-cylinder dryer. This computer program appears to be a useful and convenient tool, which allows the variation of the dryer configuration, sheet properties and process conditions. Obtained results so far appear to be acceptable in terms of physical meaning and consistency. Simulations show that moisture may be driven to the centre of the sheet, in case of strong temperature gradients and overall pressure gradients. Under certain conditions a

small underpressure in the sheet can be observed. At conditions, favourable for higher drying rates, boiling phenomena are likely to occur and may lead to relatively high gas pressures inside the sheet. In this sense it might be interesting to combine the model with a mechanical model to predict whether the sheet will withstand these internal gas pressures (delamination, blasting) or not.

In a study to compare some simulation models (Asensio, 1995) it was concluded that, though the different models were based on quite different sets of assumptions, all models yield similar predictions of the drying process. Apparently, all models have sufficient degrees of freedom to "predict" the drying behaviour. One has to be careful with the word "prediction", if model and experiment are tuned by correlations (e.g. for heat transfer). Experimental validation at the scale of an industrial dryer is quite difficult (both for technical and organisational reasons), and therefore sophisticated small scale laboratory experiments are needed in which also a lot of relevant microscopic information can be considered (e.g. NMR to validate the predicted moisture profiles).

ACKNOWLEDGMENT

The authors express their gratitude to Gerben Mooiweer for his outstanding and valuable assistance in all aspects of the programming language and the numerical library.

NOTATION

a	air content in sheet	kg air/kg dry solid
a_w	water activity	-/-
A_u , A_T , A_P	lump coefficients	(see eqns. 18-20)
d_ℓ	density of liquid water	kg water/m^3 water
D_{eff}	vapour diffusion coefficient in porous structure	m^2/s
h_ℓ , h_v	enthalpy content of liquid and vapour	J/kg
H	enthalpy content of (wet) sheet	J/kg dry solid
j_w^s , j_a^s , j_ℓ^s , j_v^s	mass fluxes of water (w), air (w), liquid water (ℓ) and water vapour (v)	kg/m^2s
k	mass transfer coefficient	m/s
K_ℓ , K_g	permeability for liquid and gas	m^2
L_u , L_T , L_P	lump coefficients	(see eqns. 12-14)
M_a , M_w	molecular weight of air (a) and water (w)	kg/mol
P	pressure gaseous phase in sheet	Pa
P_ℓ , P_c	pressure of liquid and capillary pressure	Pa
P_t	pressure of ambient air	Pa
P_v	vapour pressure	Pa
P_v^o	saturated vapour pressure	Pa
q^s	enthalpy flux with respect to solids velocity	J/m^2s
r	space co-ordinate	m
R	gas constant	J/mol K
t	time	s
T	temperature	K
u	moisture content	kg moisture/ kg dry solid
V_u , V_T, V_P	lump coefficients	(see eqns. 15-17)
z	solid co-ordinate	kg/m^2

Greek symbols

α	heat transfer coefficient	W/m^2 K
η_ℓ , η_g	dynamic viscosity of liquid and gas	Pa s

λ_{eff}	effective heat conduction coefficient of sheet	J/m s K
ν	kinematic viscosity	m^2/s
ρ_s	solids concentration	kg dry solid/m^3 tot
ρ'	density of gas phase	kg/m^3
ω_v	weight fraction of vapour in gas phase	-/-

Other subscripts

i	interface
∞	bulk
f	film layer

LITERATURE

Asensio, M.C., Seyed-Yagoobi, J., 1992, Theoretical study of single-tier versus conventional two-tiered dryer configurations, Tappi Journal, Vol. 75, nr. 10, p. 203-211.

Asensio, M.C., Seyed-Yagoobi, J., 1993, Simulation of paper-drying systems with incorporation of an experimental drum/paper thermal contact conductance relationship, Journal of Energy Resources Technology, Vol. 115, p. 291-300.

Asensio, M.C., Seyed-Yagoobi, J., Lehtinen, J.A., Karlsson, M.A., Timofeev, O.N. and Juppi, K., 1995, Comparison of several multi-cylinder paper drying simulation models, Drying Technology, Vol.13, No 4, p.945-958

Coumans, W.J., Kruf, W.M.A., 1995, Mechanistic and lump approach of internal transport phenomena during drying of paper sheet, Drying Technology, Vol. 13, no. 4, pp. 985-998

Harrmann, S. and Schulz, S., 1990, Convective drying of paper calculated with a new model of the paper structure, Drying Technology, Vol.8, No.4, p.667-703

Kruf W.M.A., 1992, The modelling of a paper dryer by using a lump model, Graduate report (in Dutch), Eindhoven University of Technology

Nissan A.H., Kaye W.G., 1955, An analytical approach to the problem of drying of thin fibrous sheets on multi-cylinder, Tappi 38:7, p.385-398.

Ramakers, B.J., 1999, A computer model for the drying of paper in a multi-cylinder paper dryer, Graduate report (in Dutch), Eindhoven University of Technology

Ramaswamy, S. and Holm, R.A., 1999, Analysis of heat and mass transfer during drying of paper/board, Drying Technology, Vol.17, no.1&2, p.49-72

Reardon, S.A., Davis, M.R. and Doe, P.E., 1999, Construction of an analytical model of paper drying, Drying Technology, Vol.17, no.4&5, p.655-690

The NAG-Fortran Library Manual – Mark 18, software edition 2.1, July 27th 1998, D03PCF.